PNC TN941 78－141

Local Flow Blockage Experiments in 37-Pin Sodium Cooled Bundles with Grid Spacers

October , 1978

POWER REACTOR AND NUCLEAR FUEL DEVELOPMENT CORPORATION

動力炉・核燃料開発事業団 (Power Reactor and Nuclear Fuel Development Corporation)

PNC TN941 78－141

October, 1978

Paper presented to the 8th Liquid Metal Boiling Working Group Meeting (Paper No. F4) held in Mol, Belgium, October 11-13, 1978

LOCAL FLOW BLOCKAGE EXPERIMENTS IN 37-PIN SODIUM COOLED BUNDLES WITH GRID SPACERS

M. Uotani, K. Haga, Y. Kikuchi* and M. Hori

Power Reactor and Nuclear Fuel Development Corporation

O-arai, Ibaraki, Japan

Abstract

A series of out-of-pile experiments were conducted on local temperature rises due to non-heat generating blockages in 37-pin bundles.

In the central blockage experiment, the central 24 subchannels of the bundle were blocked with a 5 mm thick stainless-steel plate at upstream end of a grid spacer. The blocked area was 27% of the total flow area.

In the edge blockage experiment, a stainless-steel plate blocked 39 subchannels of a 1/2 edge part of the cross-sectional area.

In both cases of the central and the edge blockage, the pin surface temperature attained a local peak in the grid spacer behind the blockage and decreased with the distance from the blockage. The mass exchange rate and the coolant residence time in the wake regions were evaluated from the observed temperature rises. The mass exchange rate per unit interface area behind the edge blockage agreed fairly well with that behind the central blockage. The dimensionless coolant residence time was found independent of Reynolds number except in the low number range, and the value obtained in the edge blockage experiment was about 2.4 times as much as that obtained in the central blockage experiment.

When experimental results were extrapolated to the reactor condition, an edge blockage of more than 30% might cause local boiling in the wake region, while a central one would not cause local boiling in any blockage ratio less than 60 %.

The temperature rises in the blocked grid spacer were also discussed.

INTRODUCTION

The problem of fuel failure propagation initiated by local flow blockage is important for safety studies relating to LMFBR. Much effort has, therefore, been made to investigate the local temperature rise due to flow blockage. The temperature rise in the downstream of a blockage depends not only on the blockage size, material and location, but also on the bundle geometry. Hence we have been conducting the experiments with electrically heated pin bundles simulating the fuel subassemblies of MONJU (Japanese prototype LMFBR). In the early

* Present address ; Kyoto University

experiment on the central blockage in a 7-pin bundle[1], it was revealed that the measured temperature rise in the downstream of the blockage agreed fairly well with the calculation with the LOCK code which was a computer program for calculating transient temperature rises due to local (up to 6 subchannels) flow blockage. In the succeeding edge blockage experiment in a 19-pin bundle[2], temperature distributions were investigated in more detail and the coolant residence time was evaluated from the temperature rises observed in the wake region.

The present experiments in 37-pin bundles have been conducted to determine the onset conditions of local boiling due to a central or an edge blockage. In addition, the measured temperature rises in the blocked grid spacer have been compared with the calculation through a simple two-dimensional analysis.

EXPERIMENTAL EQUIPMENT AND OPERATING PROCEDURES

Test Section

A series of experiments were carried out in the Sodium Boiling and Fuel Failure Propagation Test Loops, SIENA at PNC's O-arai Engineering Center.

Figure 1 shows the test section with an edge blockage. A 37-pin bundle was centered in a hexagonal tube, 50.4 mm flat-to-flat distance inside. The bundle consisted of 22 electrically heated pins within the blockage boundary and other dummy pins. The diameter of each pin was 6.5 mm and the distance between pin centers (i.e. pin pitch) was 7.9 mm. A 1/2 edge part of its cross-sectional channel area (39 subchannels) was blocked with a 5 mm thick stainless-steel plate, which was welded on the upstream side of a honey-comb type grid spacer. The detail of blocked section is shown in Fig. 2.

To keep heat losses to a minimum, the outer wall of the hexagonal tube was insulated by a compensating heater and thermal insulater.

The pin surface temperatures were measured by many chromel-alumel thermocouples of 0.3 mm in diameter, which were embedded in the outer surface of each pin. The sodium flow rates at the inlet and outlet were measured by the electromagnetic flowmeters. The output signals from the thermocouples and flowmeter were recorded on a digital data acquistion system.

The test section with a central blockage, which has already described in reference (3), had the same geometry as that with the edge blockage, except that the central 24 subchannels were blocked.

Operating Procedure

The experiments were performed in the following manner. The oxygen concentration in sodium was controlled down to 10 ppm with a purification system.

All the thermocouples were calibrated before the experiments and checked periodically during the experiments while the sodium was circulated isothermally at various temperatures. The flow rate was set and the heated pins were adjusted to the fixed power level. Sufficient time was allowed for the test section to reach steady-state conditions prior to experiments. To verify the consistency of the data, several runs were repeated.

The experimental conditions were as follows. In the central blockage experiment;

Flow velocity in normal section : 0.52∿4.16 m/s

Heat flux : 4.7∿65.0 W/cm^2
Inlet temperature : 257.8∿303.4 °C

In the edge blockage experiment;
Flow velocity in normal section : 0.48∿3.94 m/s
Heat flux : 1.0∿53.96 W/cm^2
Inlet temperature : 257.0∿299.0 °C

RESULTS AND DISCUSSIONS

Temperature Distributions

Figure 3 shows a typical radial temperature distribution in the downstream of the blockage observed in the central blockage experiment. In this figure, the horizontal axis represents the location of the thermocouples. The vertical axis shows the temperature rise of the pin surface from the inlet coolant temperature. X is the distance from the blockage. The experimental conditions were the flow velocity of 3.53 m/s (at the normal cross section) and the heat flux of 54.9 W/cm^2. It can be seen from the figure that the pin surface temperature attained a local peak in the grid spacer behind the blockage (X=12mm) and decrease with the distance from the blockage. The temperature rise of the pin surface facing the central subchannel was highest at each radial cross section behind the blockage, for the reason that the size of the blockage was rather small.

Figure 4 shows a typical radial temperature distribution observed in the edge blockage experiment. The experimental conditions are shown in the figure. As can be seen in the figure, the pin surface temperature attained a local peak in the grid spacer behind the blockage (X=12mm) and decreased with the distance from the blockage again.

The two-dimensional temperature field behind the edge blockage is shown in Fig. 5. It is seen that the temperature field was distored at the upper end of the grid due to radial flow of the recirculation. On the other hand, the pin surface temperature decreased slightly near the free edge of the blockage in the grid spacer region, which might be brought about by a little leak flow between the blockage and the pin surface.

Measured Mass Exchange Rate

The energy transfer between the wake behind the blockage and the adjacent free stream is mainly caused by the mass exchange. The following equation is, therefore, obtained from the energy conservation law in the wake region.[4]

$$\frac{dT_{WK}}{dt} = \frac{S\phi}{MC_p} - \frac{\dot{m}}{M}(T_{WK} - T_0) \qquad \text{---------(1)}$$

In the steady state condition i.e. $dT_{WK}/dt=0$;

$$\dot{m} = \frac{S\phi}{Cp(T_{WK} - T_0)} \qquad \text{---------(2)}$$

S is the sum of the heater pin surface area in the wake region. The wake regions are approximated by ellipsoids as shown in Fig. 6. In this figure, k is the ratio of the wake length to the blockage size and η is the ratio of the maximum radius of the wake region to the blockage size. Calculating the volume and interface area of the wake

region, k was assumed to be 2 for the central blockage, and 4 for the edge blockage from the hydraulic experimental results[5]. Although η is considered to be a decreasing function of the fraction of the blocked flow area[6], η was assumed to be a constant value, 1.3.

T_o was taken to be the bulk mixed mean coolant temperature at the wake region evaluated from the inlet and outlet temperatures. On the other hand, T_{WK} was the average temperature in the wake region, which did not include the grid spacer. It was calculated as the arithmetic mean of the pin surface temperature readings, which were adjusted by subtracting 'film drop', at 22mm, 32mm and 52mm downstream from the blockage for the central blockage, and at 22mm, 52mm and 82mm downstream for the edge one.

Figure 7 shows the mass exchange rates per unit interface area which were calculated from Eq. (2). The mass exchange rates per unit interface area were in proportion to the velocity at the blocked section in both cases of the central and the edge blockage, and they agreed fairly well with each other.

Dimensionless Residence Time

The coolant residence time, which was defined as the ratio of the coolant mass in the wake to the mass exchange, was evaluated from Schleisiek's equation.[7]

$$\tau \equiv \frac{M}{\dot{m}} = \frac{dh}{4} Cp \cdot \rho \frac{T_{WK} - T_o}{\phi} \qquad \text{----- (3)}$$

Figure 8 shows the effect of the flow velocity on the residence time. As can be predicted by Fig. 6, the residence time was in inverse proportion to the flow velocity at the blocked section.

Figure 9 shows the dimensionless residence time given by the following definition;

$$\tau^* \equiv \frac{\tau \cdot U_B}{D_B} = \frac{\tau \cdot U_o}{D_B \cdot (1-F)} \qquad \text{----- (4)}$$

This was deduced by G. Winterfeld to evaluate the turbulence exchange in combustion chambers and afterburners of jet engines,[8] and J.T. Han et al. applied to the blockage experiments in fuel assemblies[9]. They called it 'Blockage constant'[10]. In Eq. (4), F is the fraction of the blocked area and U_o is the velocity at normal section. D_B is the characteristic length of the blockage, which is evaluated from the following equation (see Fig. 5);

For central blockage,

$$D_B = \sqrt{\ell a \times \ell w} \qquad \text{----- (5)}$$

For edge blockage,

$$D_B = \ell a \qquad \text{----- (6)}$$

D_B for the central blockage is defined as same as that of J.T. Han et al.[9], while on the other hand D_B for the edge blockage is different from theirs.

In this figure are also shown the results for the edge blockage in the earlier 19-pin bundle experiment at PNC and for the central blockage at ORNL. It is seen that the dimensionless coolant residence time was

independent of Reynolds number except in the low number range. The decline of the value in the low Reynolds number range might be attributed to heat conduction which played an important roll only in case of low coolant velocity. Be that as it may, the dimensionless residence time could be considered to be independent of Reynolds number in the range of interest. The value obtained in the edge blockage experiment was about 2.4 times as much as that obtained in the central blockage experiment and the latter agreed well with that of ORNL.

Extrapolation to Reactor Conditions

Maximum-to-average temperature rise ratio in the wake region was obtained to estimate local temperature rise under reactor conditions. Figure 10 shows maximum-to-average temperature rise ratio for both the central and the edge blockage. In this figure, T_{max} was the maximum temperature which was measured in the wake region. It is seen that the ratio was independent of both the flow velocity and the heat flux. The value for the central blockage was 1.5, while that for the edge blockage was 1.4. The difference of the values was attributed to the fact that the axial temperature gradient in the wake region was steeper for the central blockage than that for the edge one. It is assumed here that this value is also independent of the blockage size. Following equation is obtained from the above assumption;

$$T_{max} - T_o = K \cdot (T_{WK} - T_o) \qquad \text{------ (7)}$$

where K is the maximum-to-average temperature rise ratio.

Figure 11 shows the relations between the local maximum temperature rises and the fraction of the blocked area or the blockage size, which were evaluated from eq. (3), eq. (4) and eq. (7) in full size 169-pin bundle under following conditions:

Flow velocity at normal section (U_o) : 6 m/s
Heat flux (ϕ) : 200 W/cm^2
Equivalent hydraulic diameter (dh) : 0.41 cm

The dotted line in this figure represents the flow velocity obtained in the hydraulic experiment on local blockage[5]. More than 5∿10% flow deviation was considered to be detected with an in-core flow meter, so the figure reveals that the flow blockage of more than 60% could be detected.

In both cases of the central and the edge blockage, the local temperature rise first increased with the fraction of the blocked area, and after attaining a maximum, decreased gradually. This tendency, which was similar with that evaluated by Basmer et al.[11], was ascribed to the increase of the flow velocity at the blocked section. It is seen that an edge blockage of more than 30%, which corresponds to a case that the blocked area occupied between the wrapper tube and the fifth line subchannels, might cause local boiling in the wake region, while a central one would not cause local boiling in any blockage ratio less than 60%.

Temperature Rise in Blocked Grid Spacer

From the previous discussion it might be considered that the temperature rise attained a local peak in the blocked grid spacer behind the impermeable blockage. From this reason, the necessity was felt to investigate the temperature rise in the blocked grid spacer region.

The experimental results for the edge blockage were compared with a simple two-dimensional analysis, whose description was given briefly in Appendix.

Figure 12 shows the comparison of the observed temperature rises with the calculation through the analysis at 2mm and 12mm downstream from the blockage. The calculations were performed for various velocities at the upper end of the grid spacer i.e. $U_G=0$, $U_B/4$ and $U_B/2$. As can be seen in the figure, the calculation for $U_G=U_B/2$ agreed fairly well with the observed temperature rise at X=12mm. On the other hand the calculation was higher at X=2mm. This was because the coolant flow was assumed to be one-dimensional and the effect of axial mixing was not considered in the analysis, while the coolant in the blocked grid spacer was stirred up and down.

Figure 13 shows the correlation between the fraction of the blocked area and the temperature rise in the blocked grid spacer, which was obtained from the calculation of the analysis in the case of an edge blockage. The temperature rise in the wake, shown in this figure, was used as the boundary condition. The calculation was performed for the blockage thickness of 1mm and 3mm, and for the thermal conductivity of λ_{SUS} and $\frac{1}{2}\lambda_{SUS}$, where λ_{SUS} was equivalent to the thermal conductivity of SUS316. It is seen that the coolant temperature in the blocked grid spacer exceeded the saturation temperature for an edge blockage of more than 25% when the blockage was 1mm thick, and more than 20% when it was 3mm thick. The figure also reveals, as can be predicted, that the temperature rise was heigher with lower the thermal conductivity of the blockage.

CONCLUSION

Experimental studies were carried out on local flow blockages in 37-pin sodium cooled bundles. The temperature distributions were measured in each downstream of a central and an edge blockage. The mass exchange rate and the coolant residence time were evaluated from the temperature rises in the wake regions.

Analyses of the results obtained permit the following conclusions to be drawn.

(1) In both cases of the central and the edge blockage, the pin surface temperature attained a local peak in the grid spacer behind the blockage and decreased with the distance from the blockage.

(2) The mass exchange rate per unit interface area behind the blockage agreed fairly well with that behind the central blockage.

(3) The dimensionless coolant residence time was independent of Reynolds number except in the low Reynolds number range, and the value obtained in the edge blockage experiment was about 2.4 times as much as that obtained in the central blockage experiment.

(4) When experimental results were extrapolated to the reactor condition (flow velocity of 6 m/s and heat flux of 200 W/cm^2), an edge blockage of more than 30% might cause local boiling in the wake region, while a central one would not cause local boiling in any blockage ratio less than 60%.

(5) The measured temperature rises in the blocked grid spacer were in fairly good agreement with the calculation through a simple two-dimensional analysis. The results calculated through this analysis showed that temperature rise, in the blocked grid spacer was high enough to cause sodium boiling due to an edge blockage of 20∿30%.

Local flow blockage experiments in 37-pin bundles with wire-wrapped spacers have been conducted to investigate the effect of the type of spacers. Large-scaled experiments in a 61-pin bundle are also scheduled for next year.

NOMENCLATURE

C_p ; Specific heat of sodium
D_B ; Blockage characteristic length
d_h ; Heat transfer perimeter in wake region
F ; Fraction of blocked flow area
K ; Maximum-to-average temperature rise ratio
k ; Ratio of wake length to blockage size
ℓ ; Blockage size
M ; Mass of coolant in wake region
$\dot{m}$; Mass exchange rate
Q ; Total heat input upstream from blockage
Q' ; Heat input of half cross section upstream from blockage
S ; Sum of heater pin surface area in wake region
T_o ; Average temperature in free stream surrounding wake region
T_{in} ; Inlet temperature
T_{WK} ; Average temperature in wake
T_{max} ; Maximum temperature in wake
U_o ; Flow velocity at normal section
U_B ; Flow velocity at blocked section
U_G ; Assumed flow velocity at upper end of blockage
W ; Mass flow rate
X ; Distance from blockage
η ; Ratio of maximum radius of wake region to blockage size
τ ; Coolant residence time in wake
τ^* ; Dimensionless coolant residence time
ϕ ; Heat flux

ACKNOWLEDGEMENTS

The authors wish to acknowledge the technical contributions of Mr. T. Okouchi, Mr. T. Komaba and Mr. K. Sahashi at all the stages of the experiments.

REFERENCES

(1) Y. Daigo et al. : Local Temperature Rise Due to a 6-Channel Bolkage in a 7-Pin Bundle, 6th Liquid Metal Boiling Working Group Meeting, Riseley (1975)
(2) M. Uotani et al. : Local Temperature Rise Due to 21-Subchannel Edge Blockage in a 19-Pin Bundle, Preprint 1978 Annual Meeting of the Atomic Energy Society of Japan, A47 (1978)
(3) Y. Kikuchi et al. : Temperature, Flow and Acoustic Noises in a Locally Blocked 37-Pin Bundle, 7th Liquid Metal Boiling Working Group Meeting, Petten (1977)
(4) D. Kirsch and K. Scheisiek : Flow and Temperature Distributions around Local Coolant Blockages in Sodium-Cooled Fuel Subassemblies, Progress in Heat and Mass Transfer 7 (1973)
(5) H. Nakamura : Hydraulic Simulation of Local Blockage in LMFBR Fuel Subassembly, presented at this conference.

(6) D. Kirsch : Investigations on the Flow and Temperature Distribution Downstream of Local Coolant Blockages in Rod Bundle Subassemblies, Nuclear Engineering and Design 31 (1974)
(7) K. Schleisiek : Natriumexperimente zur Untersuchung lokaler Kühlungsstörungen in brennelementähnlichen Testanordnungen, KFK 1914 (1974)
(8) G. Winterfeld : On Processes of Turbulent Exchange Behind Flame Holders, Tenth Symposium on Combustion (1965)
(9) J.T. Han, M.H. Fontana et al. : Thermal-Hydraulic of a Six-Channel Blockages in a Sodium-Cooled Simulated LMFBR Fuel Assembly, Intern. Meeting on Fast Reactor Safety and Related Physics, Chicago (1976)
(10) J.T. Han : A Model to Correlate Residence Time Measurements Behind Blockage, Trans. Amer. Nucl. Soc. 27 (1977)
(11) P. Basmer et al. : Experiments on Local Blockage, 6th Liquid Metal Boiling Working Group Meeting, Riseley (1975)

APPENDIX; ANALYSIS MODEL FOR TEMPERATURE RISE IN BLOCKED GRID SPACER

Figure 14 shows the geometrical configuration considered in the simple two-dimensional analysis. The grid spacer and the blockage were divided into equal parts respectively in axial direction and into each subchannels radially.

There was a slit at each side of the grid spacer as shown in figure 2. The coolant could flow into an adjacent subchannel through the slit, but the complicated flow was simplified as follows. At the upper end of the grid spacer the coolant flew toward the free edge of the blockage from the wrapper wall side, and at the bottom of the blocked grid the coolant might stand still. Hence the linear flow distribution was assumed in the grid region as shown in Fig. 14. The downward flow was also assumed at the adjacent subchannel to the wrapper tube.

Two-dimensional heat balance equations, in which convections by the one-dimensional flow were considered, were deduced under the following boundary condititons.

(A) Inner wall of wrapper tube faced to the wake

----- $T = T_{WK}$

(B) Upper end of the grid spacer

----- $T = T_{max} = K(T_{WK}-T_o) + T_o$

(C) Upstream side of the blockage

----- $T = T_{in} + Q'/C_{p\gamma}(\frac{W}{2})$

(D) Free edge of the blockage

----- $T = T_{in} + Q/C_p \cdot \gamma \cdot W$

(E) Outer wall of the wrapper tube

----- No heat dissipation

Equations were solved by using S.O.R. method.

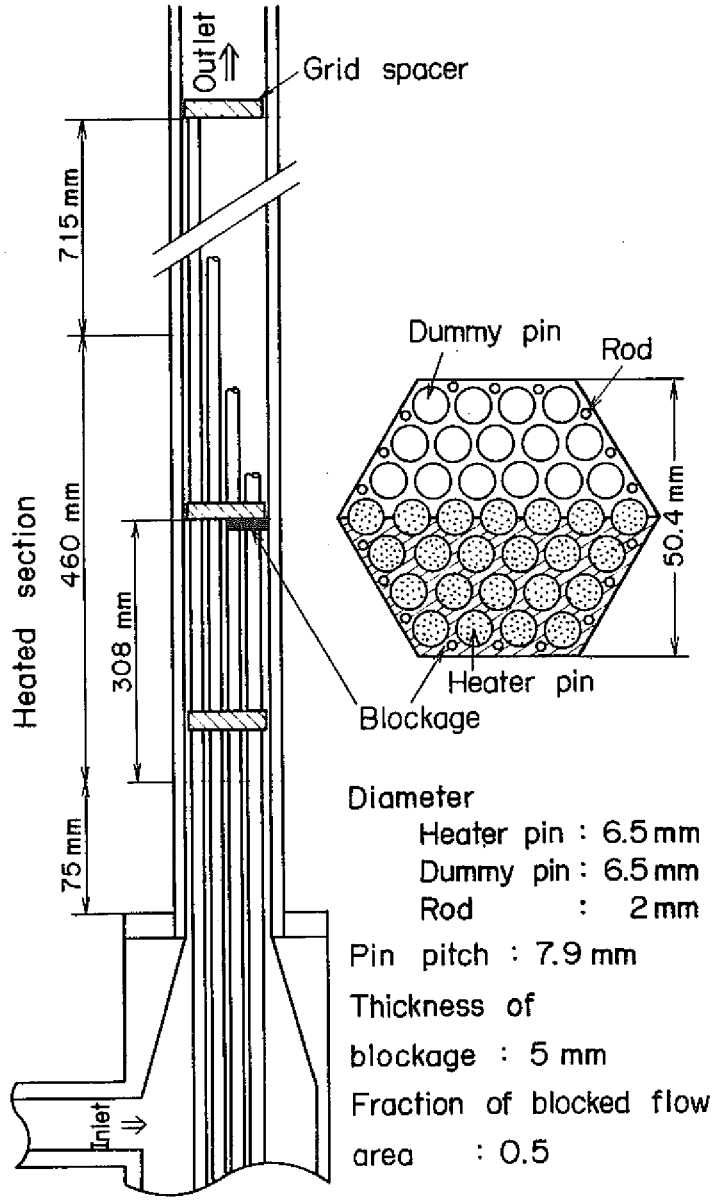

Fig. 1 Locally blocked 37-pin bundle test section

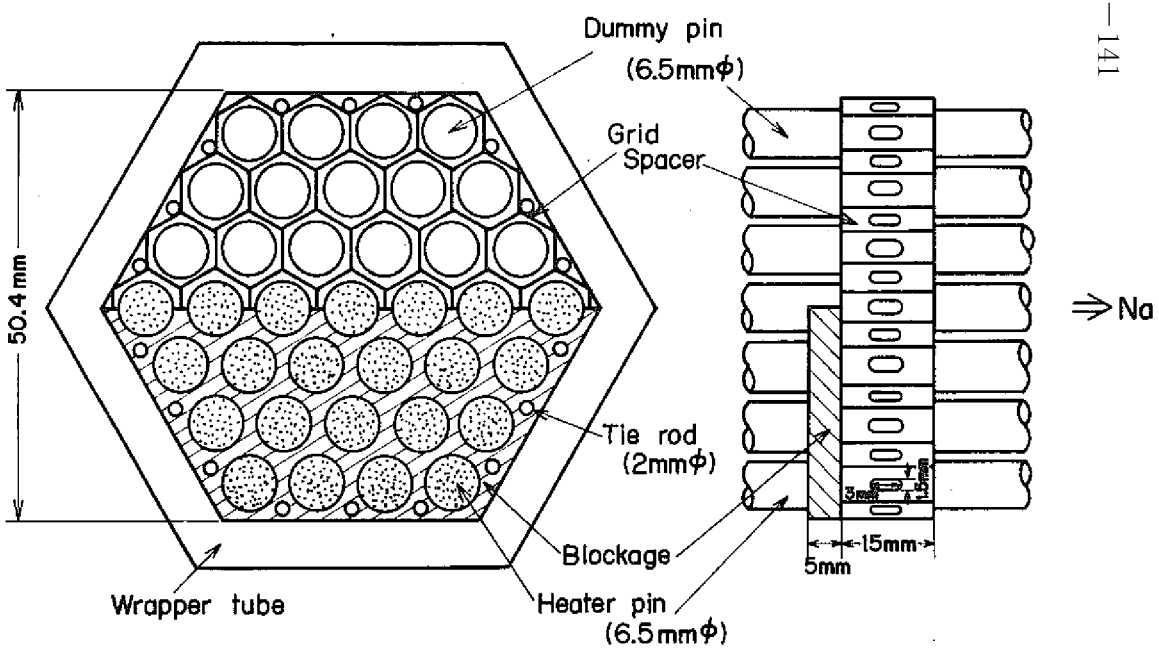

Fig. 2 Detail of blockage section

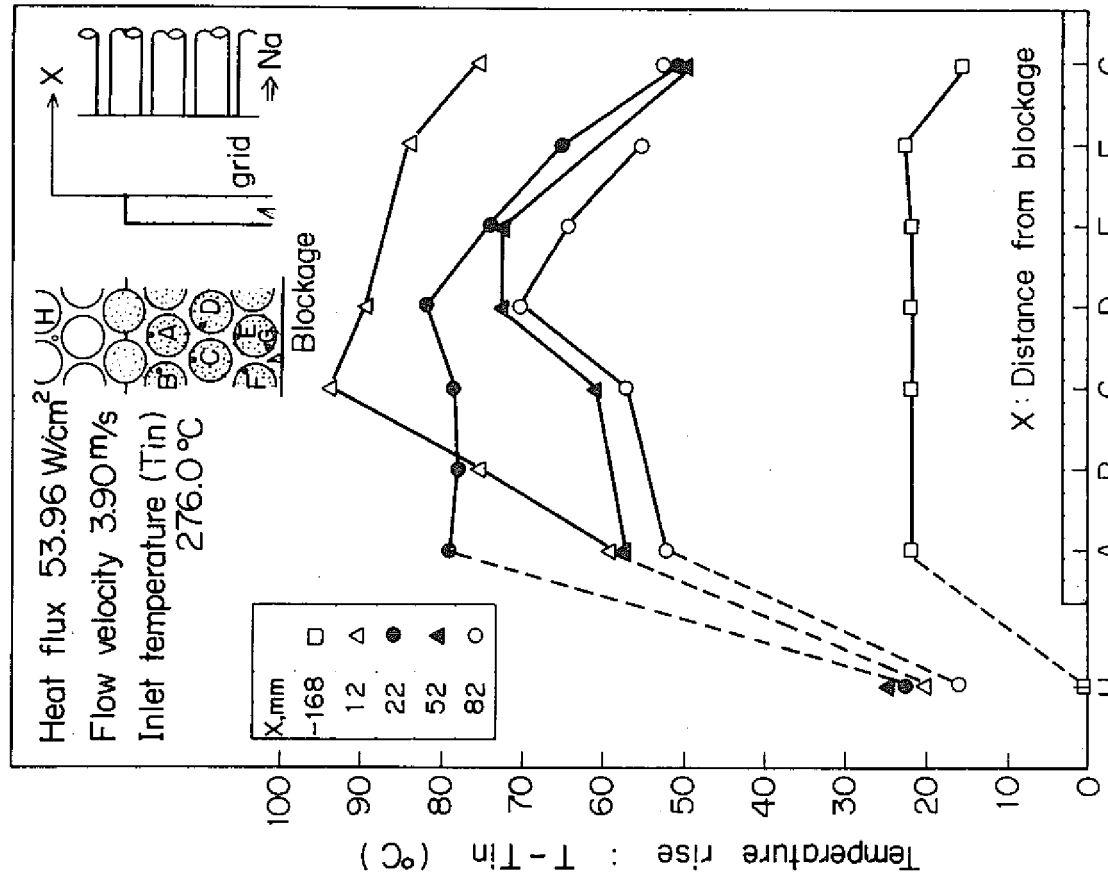

Fig. 4 Radial temperature distribution in downstream of blockage observed in experiment

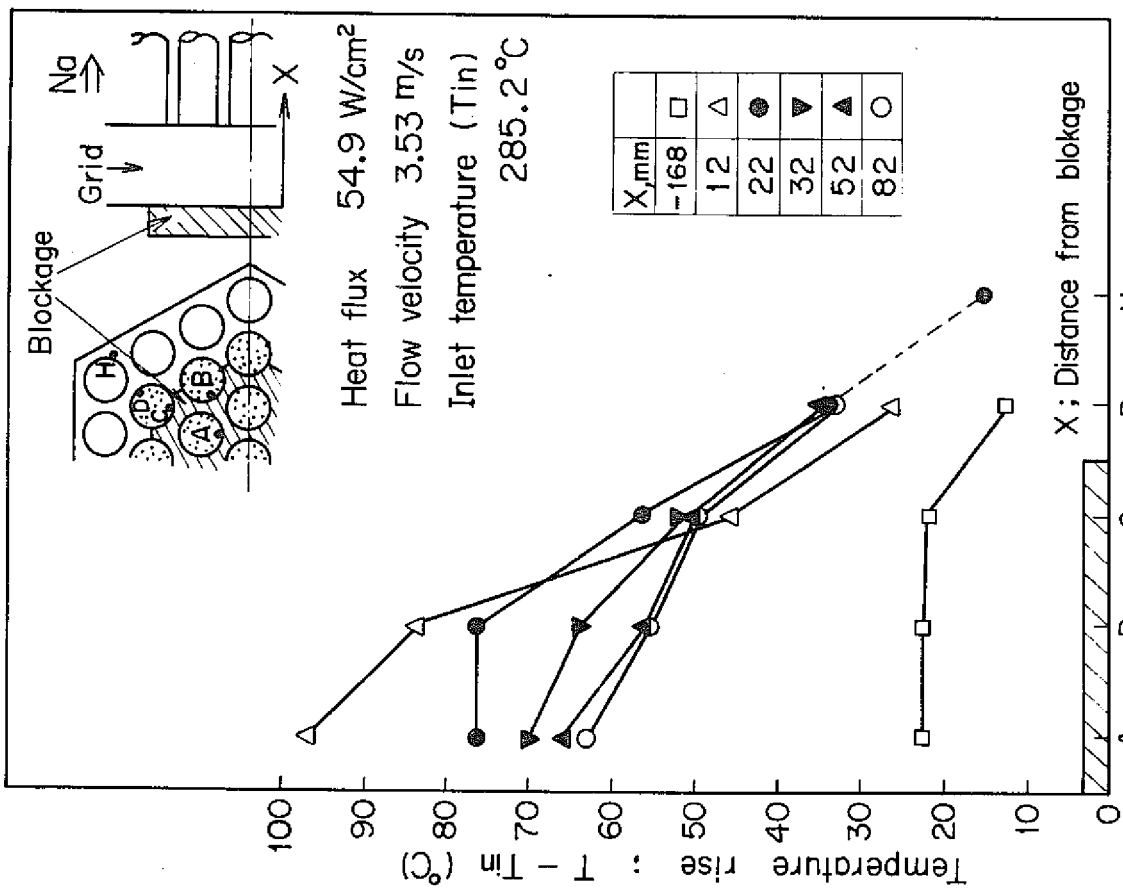

Fig. 3 Radial temperature distribution in downstream of blockage observed in the central blockage experiment

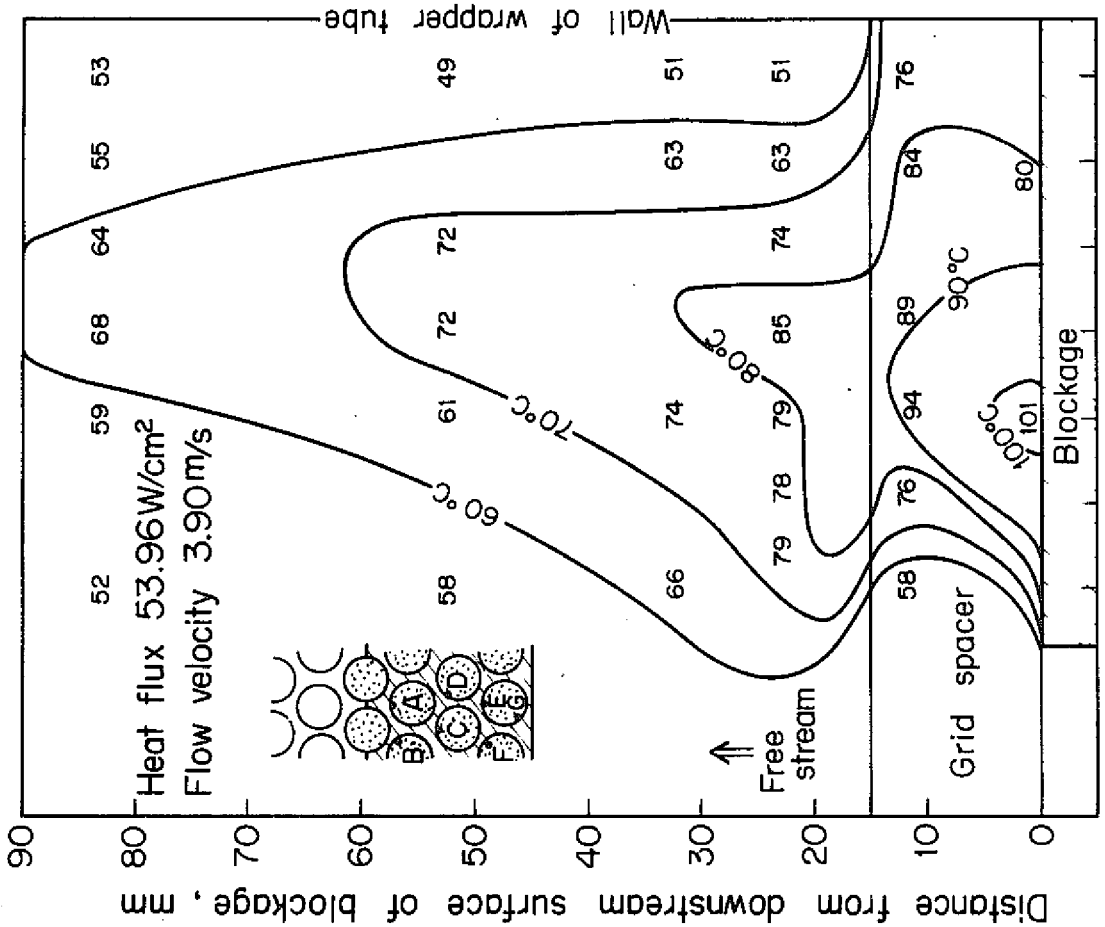

Fig. 5 Temperature field behind the blockage observed in experiment

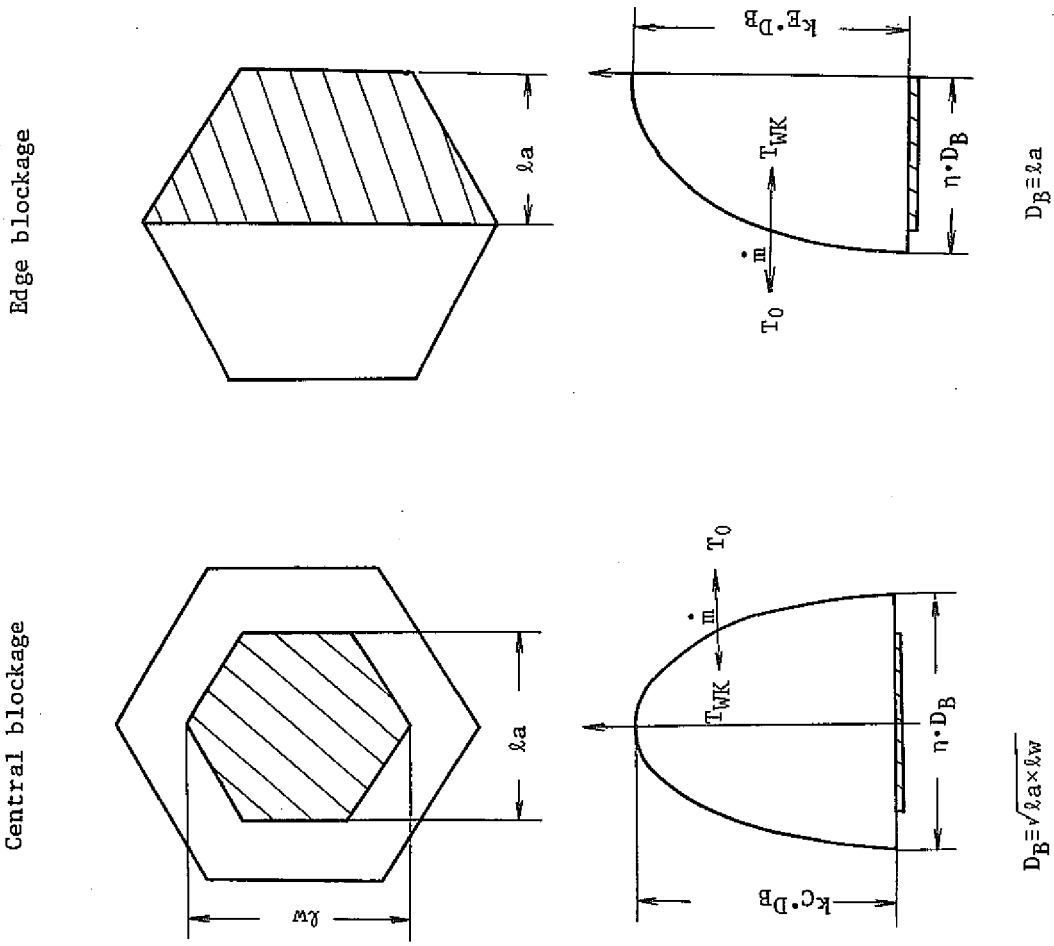

Fig. 6 Wake regions for the central and the edge blockage

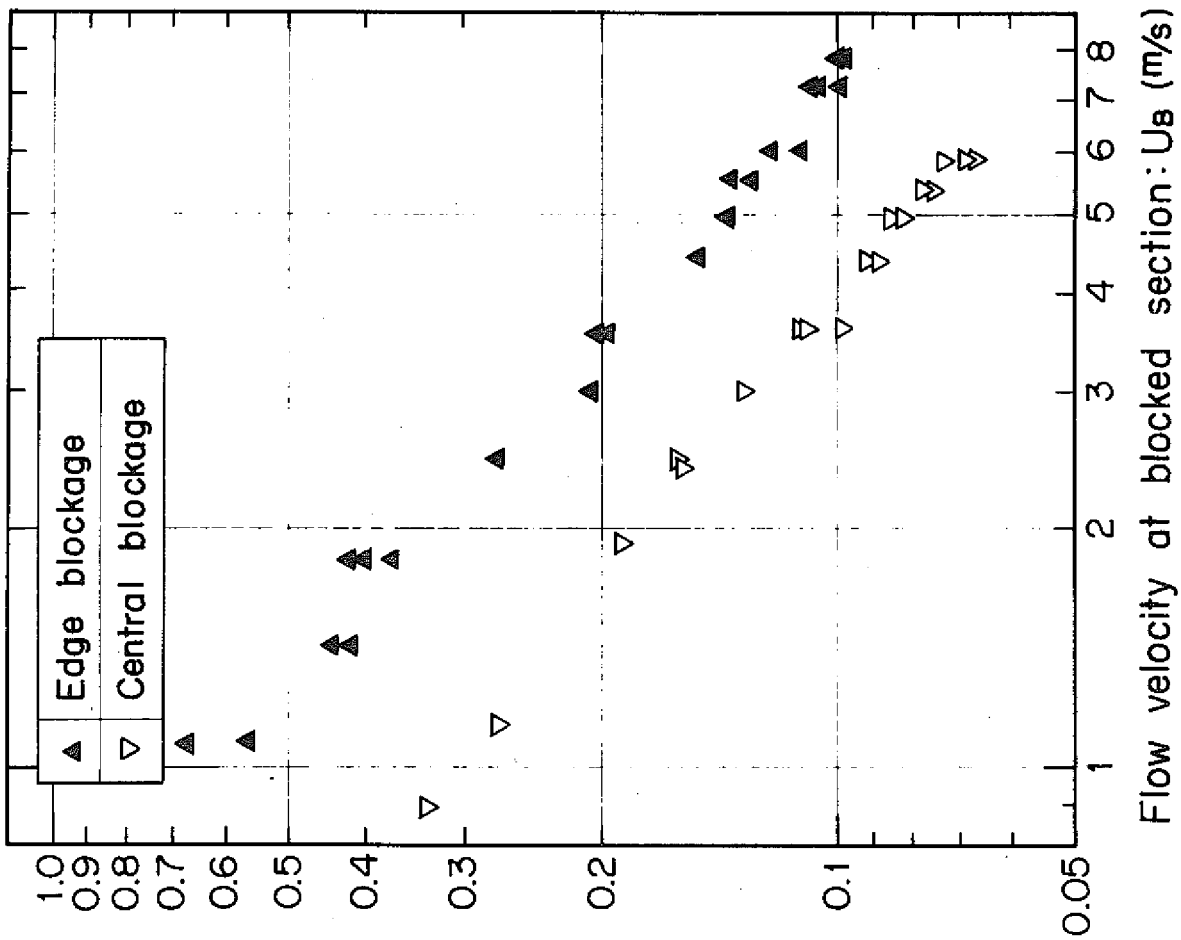

Fig. 8 Relation between residence time and flow velocity

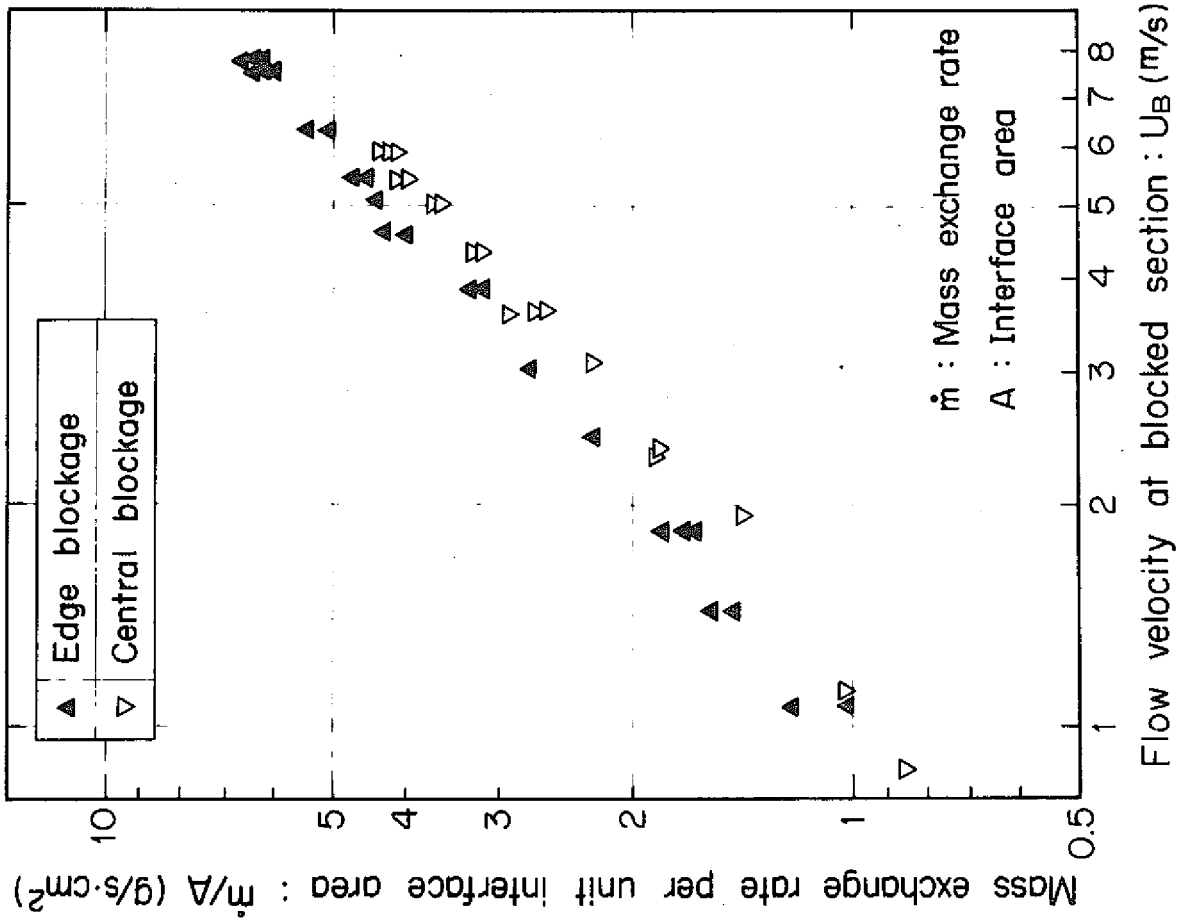

Fig. 7 Mass exchange rate per unit interface area for the wake behind blockage

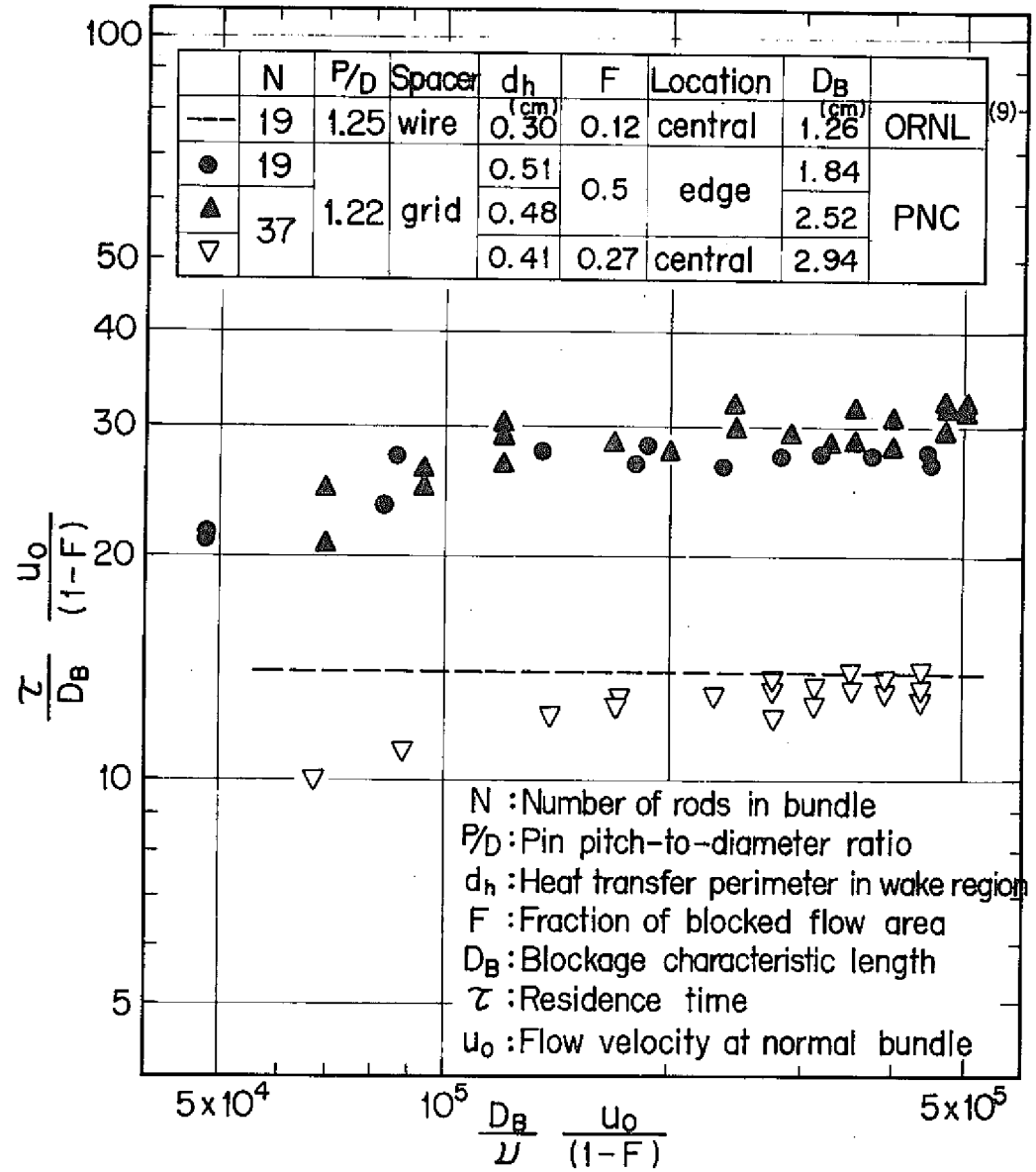

Fig. 9 Relation between dimensionless fluid residence time and Reynolds number

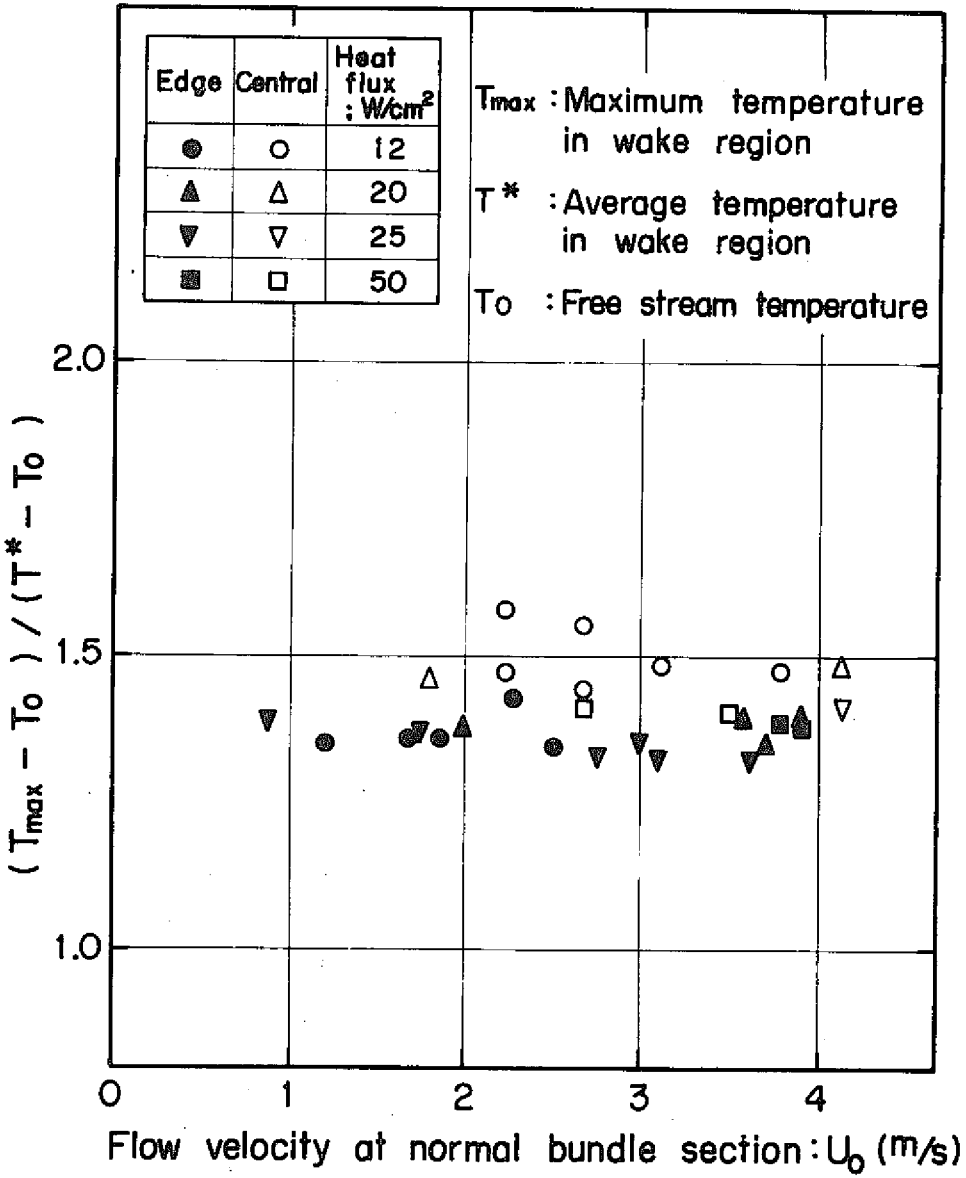

Fig. 10 Ratios of maximum wake temperature rise to average wake temperature rise

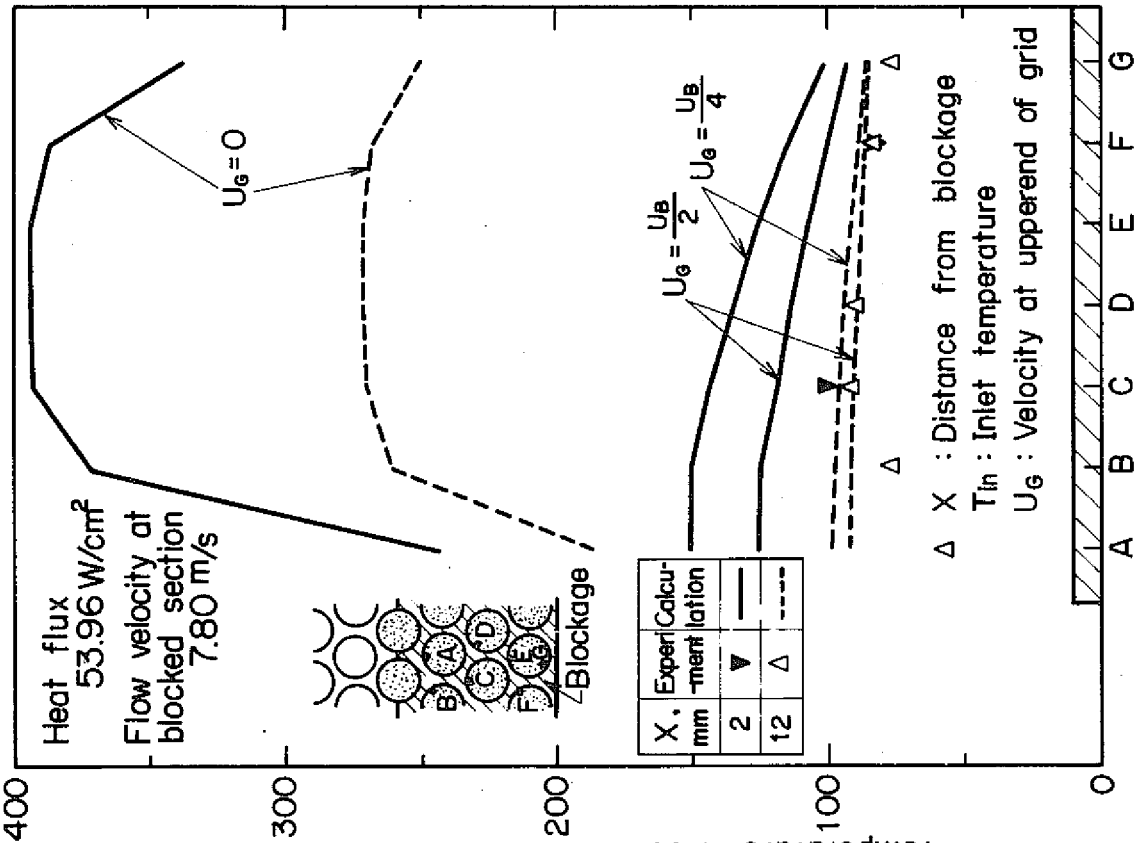

Fig. 12 Comparison of measured temperature rise in blocked grid spacer with calculation by simple two-dimensional model analysis

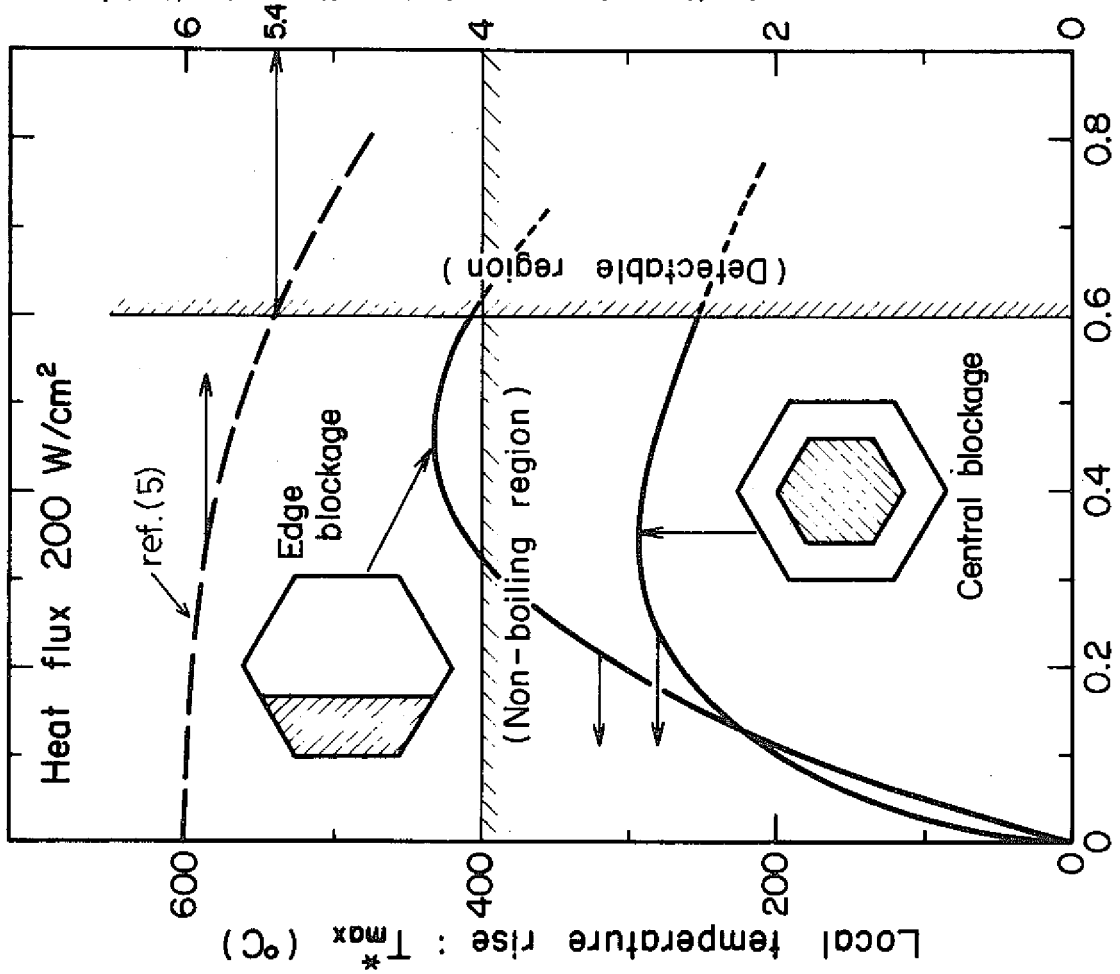

Fig. 11 Relation between local temperature rise in wake region and fraction of blocked flow area

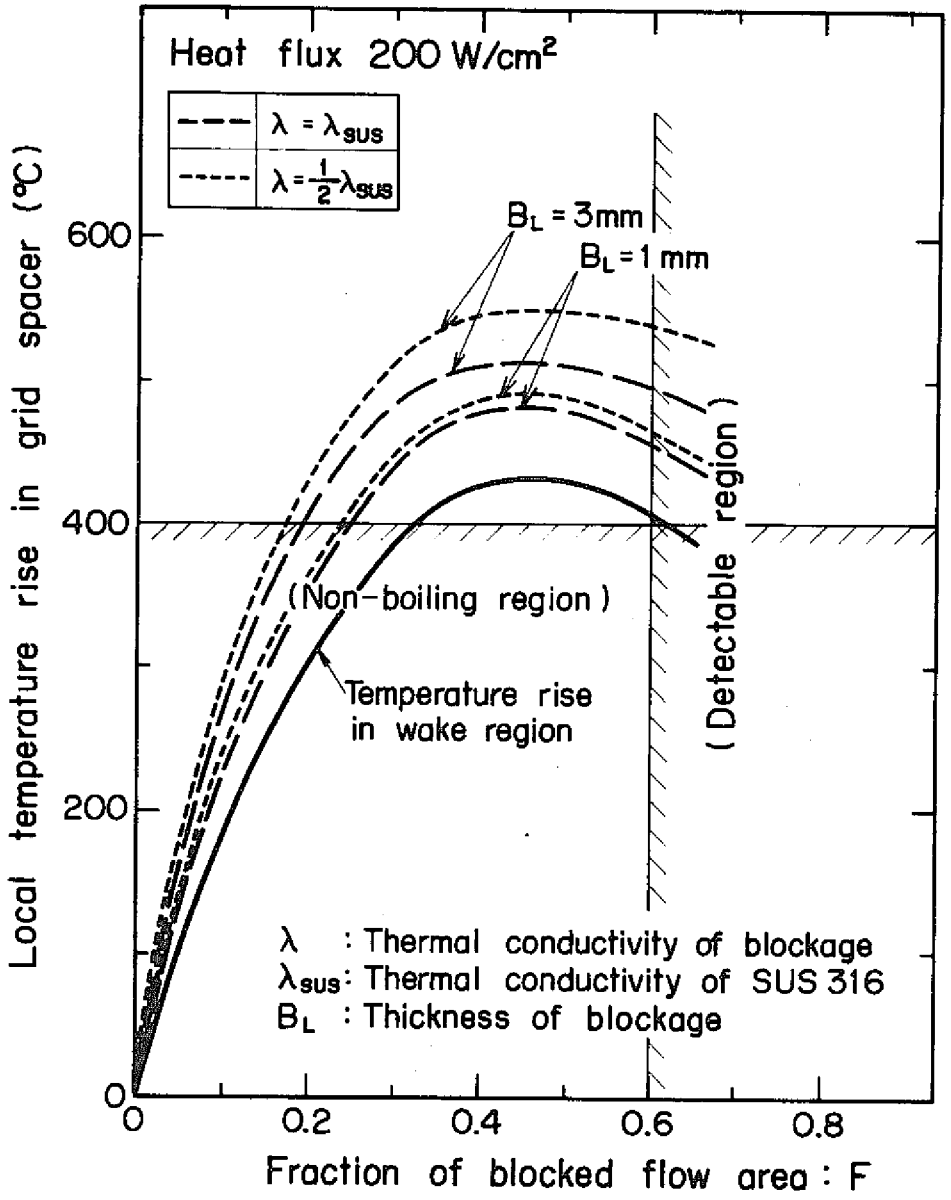

Fig. 13 Local temperature rise in blocked grid spacer calculated by simple two-dimensional model analysis

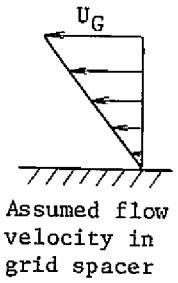

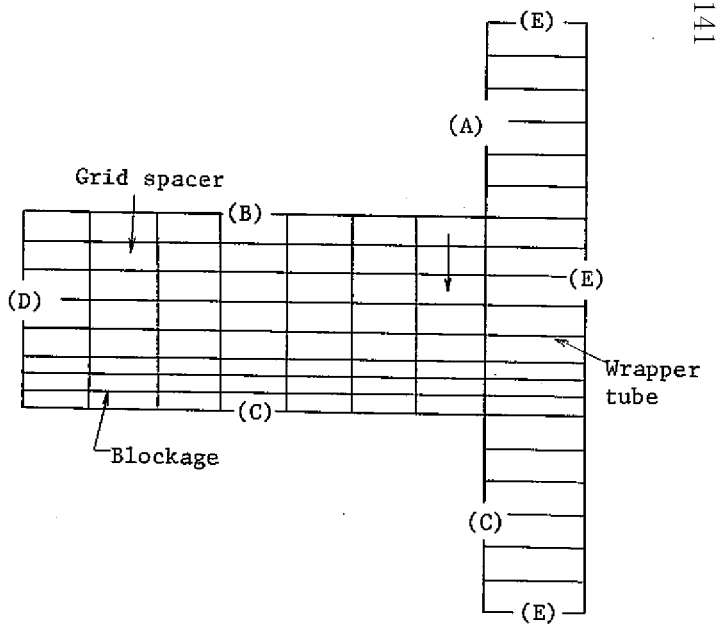

Fig. 14 Geometrical configuration considered in simple two-dimensional analysis